LEGIBILITY NOTICE

A major purpose of the Technical Information Center is to provide the broadest dissemination possible of information contained in DOE's Research and Development Reports to business, industry, the academic community, and federal, state and local governments.

Although portions of this report are not reproducible, it is being made available in microfiche to facilitate the availability of those parts of the document which are legible.

3

LA-UR-88-669

CONF-8804104--6

Los Alamos National Laboratory is operated by the University of California for the United States Department of Energy under contract W-7405-ENG-36

TITLE HIGH-ENERGY LASER-ASSISTED IMAGING THROUGH VAPORIZING AEROSOLS

LA-UR--88-669

DE88 007911

AUTHOR(S) A. ZARDECKI, T-DOT
S.A.W. GERSTL, T-DOT

SUBMITTED TO FOR PRESENTATION AT THE SPIE 88 TECHNICAL SYMPOSIUM ON OPTICS, ORLANDO, FLA., APRIL 4-8, 1988 AND TO BE INCLUDED IN THE PROC. OF THIS MEETING

FEBRUARY 1988

DISCLAIMER

Los Alamos Los Alamos National Laboratory
Los Alamos, New Mexico 87545

High-energy laser-assisted imaging through vaporizing aerosols

A. Zardecki and S. A. W. Gerstl

Theoretical Division, Los Alamos National Laboratory
Mail Stop K723, Los Alamos, NM 87545

ABSTRACT

The degradation of image quality due to multiple scattering in a turbid medium is analyzed under various conditions of illumination. The emphasis is on the forward-peaked multiple scattering effects, which can adequately be described by the small-angle approximation. In the case of incoherent illumination, the modulation transfer function (MTF) can be given explicitly both in the low- and high-frequency limits. For scattering with smaller degree of anisotropy, the MTF should be computed numerically by considering solutions to the equation of radiative transfer with a line or point source. As the beam power increases, the turbid medium becomes modified by its interactions with the beam, thus affecting the image resolution. In this nonlinear transport regime (flux levels of the order of 10^6 W/cm^2 and higher) the propagation leads actually to beam narrowing. In the context of the imaging problem, an apparent paradoxical situation—in which the image of a point source narrows down as the high-energy laser (HEL) beam propagates—is discussed.

1. INTRODUCTION

If a laser beam is used to illuminate an object, the radiation in the image plane is perturbed by an interposed medium, e.g. haze, smoke, or water cloud. For linear turbid media, encountered in the propagation of solar radiation and low-energy laser beams, the degradation of image quality can be analyzed within the framework of the small-angle approximation,[1-3] the diffusion approximation,[4] or a rigorous two-dimensional radiative transfer equation.[5] These three approaches allow us to highlight different aspects of the imaging problem when multiple scattering effects are important.[6]

Experimental evidence, as shown by Kopeika[7-9] and Kuga and Ishimaru,[2,3] indicates that—in addition to turbulence—the multiple scattering from discrete particles seriously limits image resolution. If particles are larger than or comparable to the wavelength of radiation, the use of the small-angle approximation leads to extension of earlier classic results to a wider class of fields satisfying a factorization condition.[10] These are, in general, the partially coherent radiation fields. In the incoherent illumination limit, the MTF can be derived in a closed form, provided the scattering phase function is forward peaked. Otherwise, with the aid of a solution to the equation of radiative transfer corresponding to an isotropic line source, the MTF is computed numerically.

Performance of tracking systems has explicitly been associated with the properties of target signatures,[11] and implicitly with the properties of the intervening medium. For HEL beams, the scattering and absorption cross sections of the medium vary with the value of the radiation flux; the beam propagation becomes nonlinear. If the irradiance does not exceed a flux density of 10^5-10^6 W/cm,^{2} the power loss of the beam is controlled by the process of aerosol vaporization. The coupled aerosol-beam equations, in which the dominant interactions are diffusive mass transport and conductive energy transport, are solved numerically to obtain the spatio-temporal behavior of the propagating beam and irradiated aerosols. The spatial broadening of a localized laser disturbance allows us to study the nonlinear response function of the irradiated medium when the information is transmitted from the object to the image plane. In the frequency domain, a quantity analogous to the MTF is obtained. Interestingly, in the limit of linear interactions, the MTF of the incoherent illumination is recovered. The point spread function shows less and less broadening as the laser energy increases, the process we term HEL-assisted imaging. If aerosol cloud clearing occurs, essentially no spatial frequencies are lost in the image plane.

2. CONDITIONS OF ILLUMINATION

Let a beam of light propagate along the positive direction of the z-axis, with the space between the object plane and the image plane filled by a turbid medium. To specify the location in the plane z = const, we use together with variables ρ_1 and ρ_2 the central $\rho_c = (\rho_1 + \rho_2)/2$ and difference $\rho_d = \rho_1 - \rho_2$ variables. If $u(\rho, z)$ is a complex function representing the disturbance of an electromagnetic field in the scalar approximation and $I(\rho, z, \phi)$ denotes the radiance distribution function, then the mutual coherence function $\Gamma(\rho_1, \rho_2, z) = < u(\rho_1, z)u^*(\rho_2, z) >$ is related to I by[12]

$$\Gamma(\rho_1, \rho_2, z) = \int I(\rho, z, \phi) exp(ik\phi \cdot \rho_d) d^2\phi, \tag{1}$$

where k is the wave number of radiation.

Equation (1) implies that the incoherent mutual coherence function $\Gamma(\rho_1, \rho_2, z) = (4\pi^2/k^2) I(\rho_1, z)\delta(\rho_1 - \rho_2)$ corresponds to the isotropic radiance $I(\rho, z, \phi) = I(\rho_c, z)$. On the other hand, the Gaussian distribution function

$$I_0(\rho_c, \phi) = (\beta^2\gamma^2/\pi^2) exp(-\beta^2\phi^2 - \gamma^2\rho_c{}^2), \tag{2}$$

in the plane $z = 0$, corresponds to the coherent illumination; the mutual coherent function $\Gamma(\rho_1, \rho_2)$ factorizes if we identify γ with k/β.

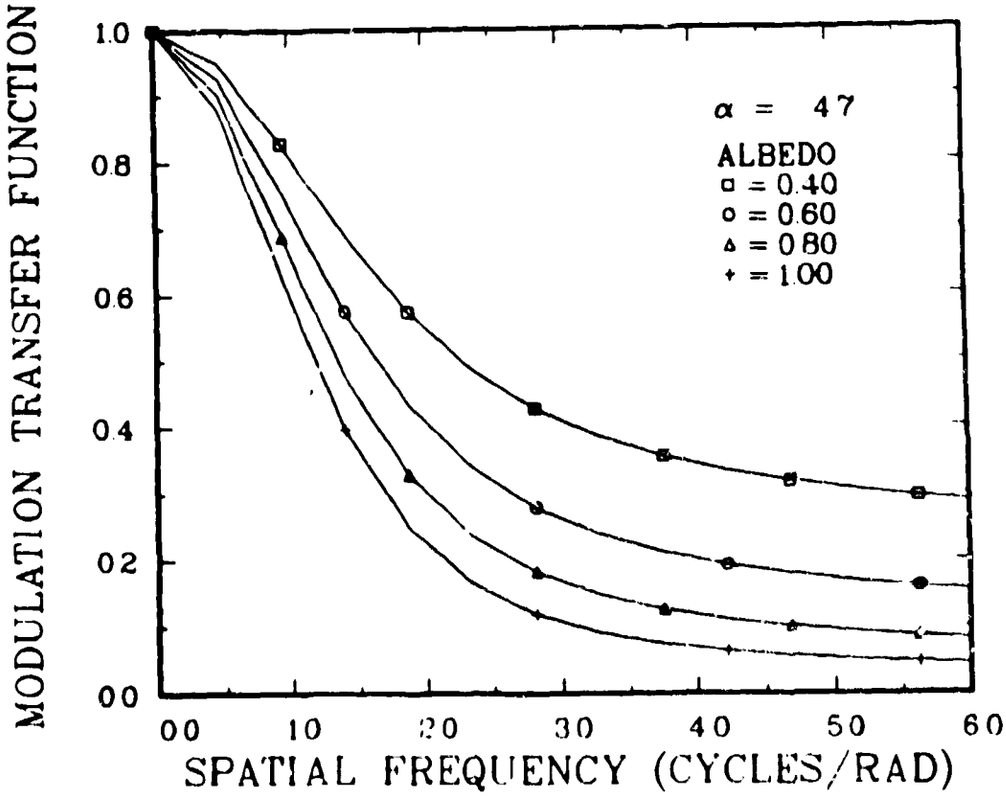

Figure 1 Small-angle approximation MTF for optical depth $\tau = 4$, and $\alpha = 4.7$ rad^{-1}

In the next section, we recall the formula for the MTF corresponding to the incoherent, delta correlated, radiation field

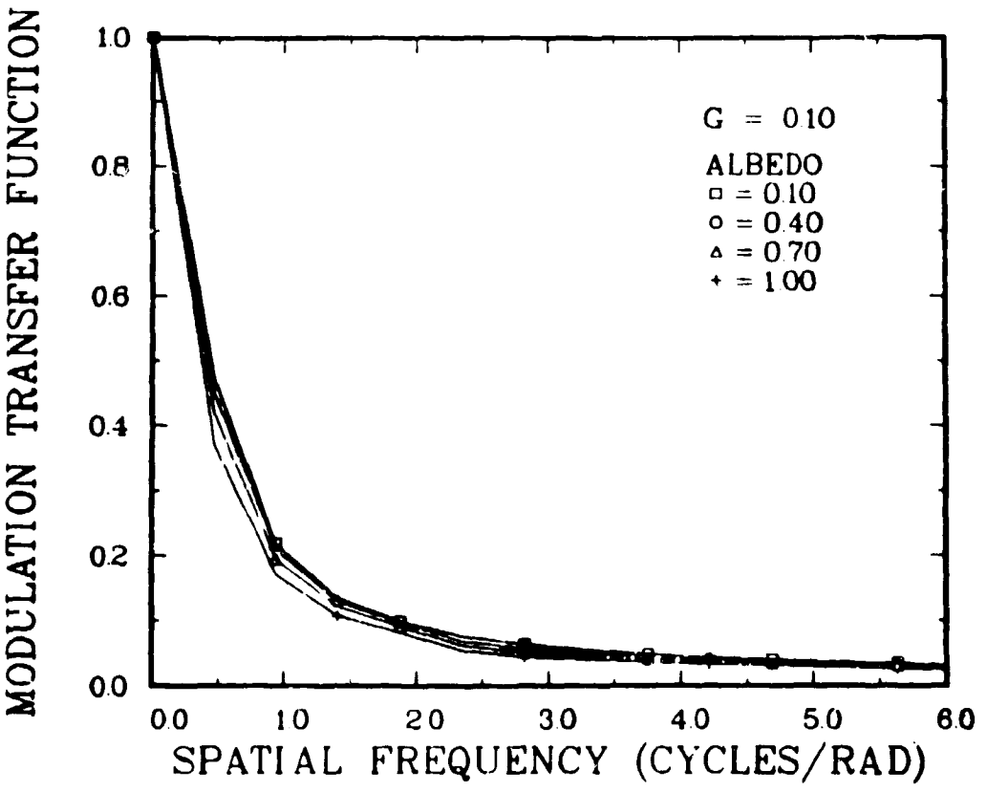

Figure 2. MTF as computed with TWOTRAN code. Asymmetry factor g = 0.1, $\tau = 1$.

3. MTF FOR THE LINEAR MEDIUM

When particle size is much greater than a wavelength, the wave scattered by particle is largely confined within a small angle in the forward direction, resulting in the simplification of the propagation laws for the radiance and mutual coherence function. We assume the homogeneous medium to be specified by the volume extinction and scattering coefficients, σ_t and σ_s, and the single scattering phase function, taken for convenience[13] as a Gaussian function with the parameter α:

$$p(\phi) = \frac{\alpha^2}{\pi} exp(-\alpha^2\phi^2). \tag{3}$$

Under the small angle-approximation, the propagation law for the mutual coherence function, combined with the condition of isoplanatism, leads to the MTF of the form

$$M(f) = exp\left[\sigma_a z - \sigma_t z + \frac{\sigma_s z \alpha}{2\sqrt{\pi} f} erf\left(\frac{\pi f}{\alpha}\right)\right]. \tag{4}$$

Here the spatial frequency f is expressed in cycles per radian of field of view, $\sigma_a = \sigma_t - \sigma_s$, and erf denotes the standard error function. As illustrated in Fig. 1, in which the MTF is shown for different single scattering albedos $\omega = \sigma_s/\sigma_t$, Eq. (4) predicts correctly the Gaussian roll off for low spatial frequencies, and the leveling of the MTF as $f \to \infty$. The MTF rolls off at spatial frequency $f_r = (\alpha/\pi)(3/\tau_s)^{1/2}$, where $\tau = \sigma_t z$ is the optical depth, whereas $\tau_s = \sigma_s z$ is the scattering optical depth. For moderate values of τ_s and α, f_r can be quite small, reaching a few cycles per radian. Provided a good Airy pattern can be obtained, this does not imply, however, the deterioration of the image.

When the scattering becomes isotropic, the forward scattering approximation breaks down, and one is forced to seek numerical solutions to the imaging problem. This has been done in the past both by applying the rigorous equation of transfer (only 2-D algorithms are of practical value) and by employing the diffusion approximation. Figure 2 shows the MTF computed with the aid of the TWOTRAN transport code,[5] in which the radiation from a line source propagates through a nearly isotropic medium, with the asymmetry factor (average cosine of the scattering angle) $g = 0.1$. In this regime, especially for $\omega \leq 0.8$, the radiative transport approach seems to be the only feasible tool of computing the MTF.

4. IMAGING THROUGH THE NONLINEAR MEDIUM

The time-dependent radiative transfer equation, written in the small-angle approximation, has the form

$$\left(\frac{\partial}{\partial z} + \phi \cdot \frac{\partial}{\partial \rho} + \sigma_t\right) I(\rho, z, \phi, t') = \sigma_s \int p(\phi - \phi') I(\rho, z, \phi', t') d^2\phi'. \tag{5}$$

In Eq. (5), $t' = t - z/c$ is the retarded time; the properties of the medium will, in general, be dependent on space and time.

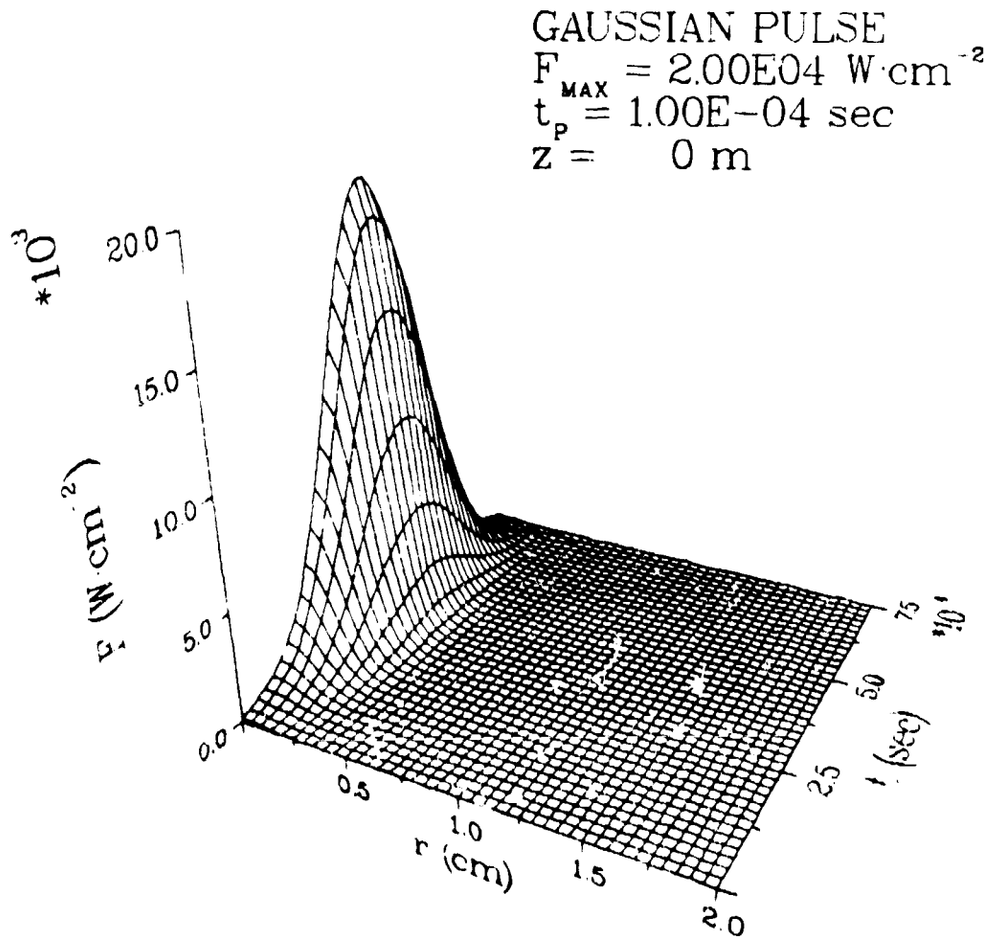

Figure 3. Functional shape of the laser pulse in the input plane, $z = 0$. The independent variables are time t and radial distance r from the beam axis; the latter is denoted ρ in the text. Peak power $F_{MAX} = 2 \times 10^4$ W/cm^2.

The solution algorithm for Eq. (5) is given in Ref. 14. For the sake of completeness, we provide the final formulas for the laser flux (irradiance) in the case where the phase function is described by Eq. (3) and where the pulse profile at $z = 0$ factorizes

$$I(\rho, z = 0, \phi, t) = I_0(\rho, \phi)T(t), \tag{6}$$

where the prime over t nas been dropped. The small-angle approximation irradiance

$$F(\rho, z, \tau) = \int I(\rho, z, \phi, \tau)d^2\phi \tag{7}$$

is obtained by successively applying the formula

$$F(\rho, z + \Delta, \tau) = \frac{1}{(2\pi)^2} exp[-\sigma_t(z, \tau)\Delta] \int G(\rho - \rho', z, \tau)F(\rho', z, \tau)d^2\rho'. \tag{8}$$

Here Δ is a propagation distance satisfying the condition $\sigma_s\Delta \ll 1$, and the propagation kernel G is defined as

$$G(\rho, z, \tau) = \frac{1}{\pi}[K^{-1}exp(-\rho^2/K) + \sigma_s\Delta L^{-1}exp(-\rho^2/L)]; \tag{9}$$

the parameters K and L are expressed in terms of α, the inverse angular spread of the phase function, and β, the inverse angular spread of the beam,[14] as

$$K(z) = 2z\Delta/\beta^2, \tag{10}$$

$$L(z) = 2z\Delta/\beta^2 + \Delta^2/\alpha^2. \tag{11}$$

In actual computations, the algorithm is further improved if we let the values of σ_s, σ_t, and α be induced by the spatial beam profile. We note that Eqs. (10) and (11) simplify in the limit of a collimated beam, when $\beta \to \infty$. In the remaining part of this section, we sketch the derivation of the response to a spatially narrow collimated beam, assuming the limiting case of constant medium parameters. This assumption will be valid only when the incident beam is of sufficiently low flux, i.e. when the propagation is linear.

The irradiance distribution function in the input (object) plane corresponding to the radiance I_0 given by Eq. (2) is

$$I(\rho, t) = T(t)\frac{\gamma^2}{\pi}exp(-\gamma^2\rho^2). \tag{12}$$

We now divide the scattering medium into infinitesimal slabs, each of width $\Delta^{(k)}, k = 1, 2, \ldots$, at z_k, and apply succesively Eq. (8) to propagate radiation over the extent of each slab. For homogeneous medium, Δ in Eq. (10) may be replaced by z, leading to

$$I(\rho, z, t) = T(t)\{\frac{\gamma^2}{\pi}exp(-\gamma^2\rho^2) + \frac{1}{\pi}\sum_k \gamma_k{}^2 exp(-\gamma_k{}^2\rho^2)\sigma_s\Delta^{(k)}\}exp(-\sigma_t\Delta^{(k)}), \tag{13}$$

where

$$\gamma_k{}^2 = \frac{\gamma^2}{1 + \gamma^2 z_k{}^2/\alpha^2}. \tag{14}$$

In the (spatial) frequency domain, the Fourier transform theorem yields

$$\hat{I}(f, z, t) = T(t)exp(-\frac{f^2}{4\gamma^2})[1 + \sum_k exp(-\frac{f^2 z_k{}^2}{4\alpha^2})\sigma_s\Delta^{(k)}] \sum_k exp(-\sigma_t\Delta^{(k)}), \tag{15}$$

When the expression in square brackets in Eq. (15) is replaced by an exponential, and the summation is converted to integration, we obtain

$$\hat{I}(f) = T(t)exp(-\frac{f^2}{4\gamma^2})M(f), \tag{16}$$

with $M(f)$ given by Eq. (4). We see that although the laser beam corresponds to the coherent illumination, the propagation of irradiance is still described in terms of the MTF of the incoherent illumination, provided that the parameters of the medium do not change. For higher fluxes, we solve numerically our propagation algorithm, together with appropriate equations for the vaporizing aerosol particles.

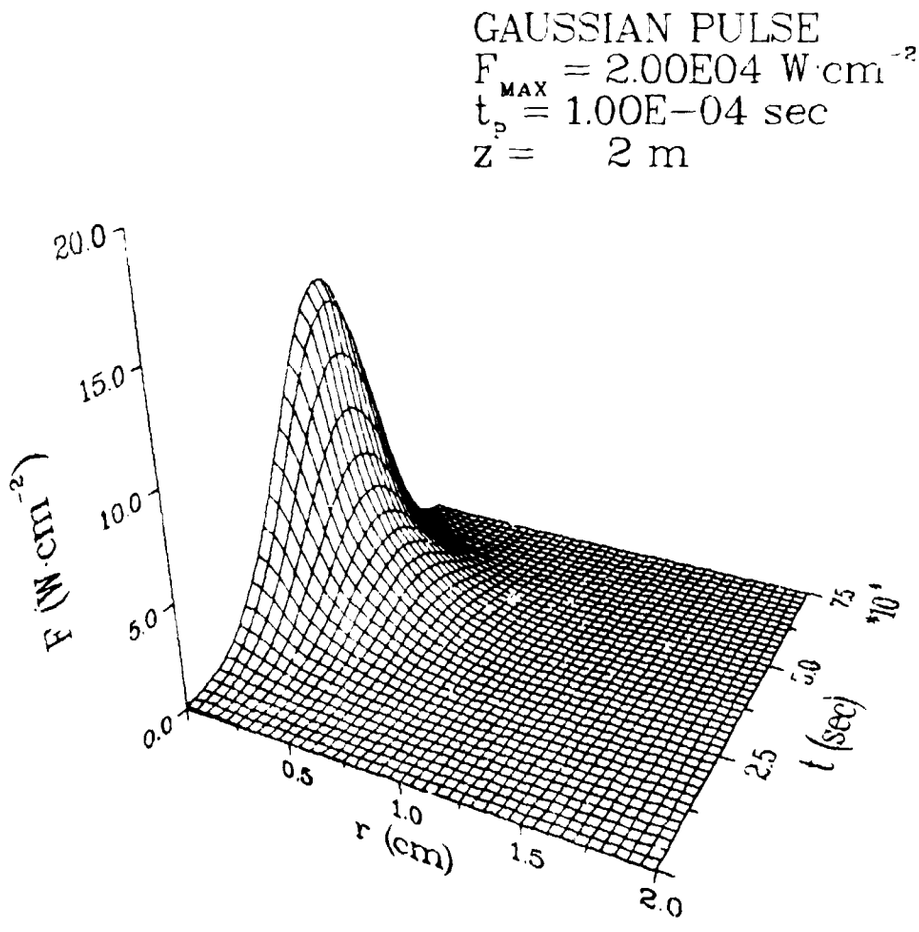

Figure 4. Functional shape of the pulse shown in Fig. 3 at a distance $z = 2$ m.

5. NUMERICAL RESULTS

To illustrate the foregoing considerations, we choose the medium in the form of a 3 m wide slab, initially filled with a monodisperse collection of 10 μm radius water droplets. The concentration of the droplets $n_0 = 3.75\times10^3$ cm^{-3} corresponds to the optical depth $\tau = 8.25$ at the laser wavelength $\lambda = 3.8$ μm. The laser beam having the initial spot size of 0.2 cm propagates in the form of a pulse of 0.1 msec duration. The two flux levels we consider are $F_1 = 2.0\times10^4$ W/cm^2 and $F_2 = 2.0\times10^6$ W/cm^2; both values define the peak flux at the center of the pulse. While the former value defines the linear regime, the latter one leads to nonlinear propagation effects induced by the vaporization of water droplets. In Figs. 3 and 4, we show the spatio-temporal shape of the pulse for $z = 0$ (input plane) and $z = 2$ m. It is seen that, in addition to the pulse attenuation, there is a spatial broadening produced by the multiple scattering. To gain a better insight into the physics involved here, we show in Fig. 5 the on-axis pulse attenuation as a function of time and propagation distance. The corresponding change in the droplet radius is depicted in Fig. 6. Figure 7 shows the Fourier transform of the spatial pulse shape, termed "modulation transfer function," for different path lengths. We stress that, due to the nonlinear nature of the propagation process, the resemblance to the MTF of linear optics is only formal. The results of Fig. 7 should be compared to those of Fig. 8, in which the MTF is computed directly from Eq. 4 of Sec. 3.

The results of computation in the nonlinear regime are depicted in Figs. 9–12. As is evident from Figs. 9 and 10, in the process of propagation the pulse suffers spatial narrowing, accompanied by the punch through effect, in apparent violation of the Beer-Lambert law. Figure 11, which shows the droplet radius as a function of time and longitudinal distance, explains the effect in terms of the droplet vaporization.[14] The nonlinear MTF, shown in Fig. 12, illustrates a new effect that we term HEL-assisted imaging. The spatial frequency rolls off at much larger values

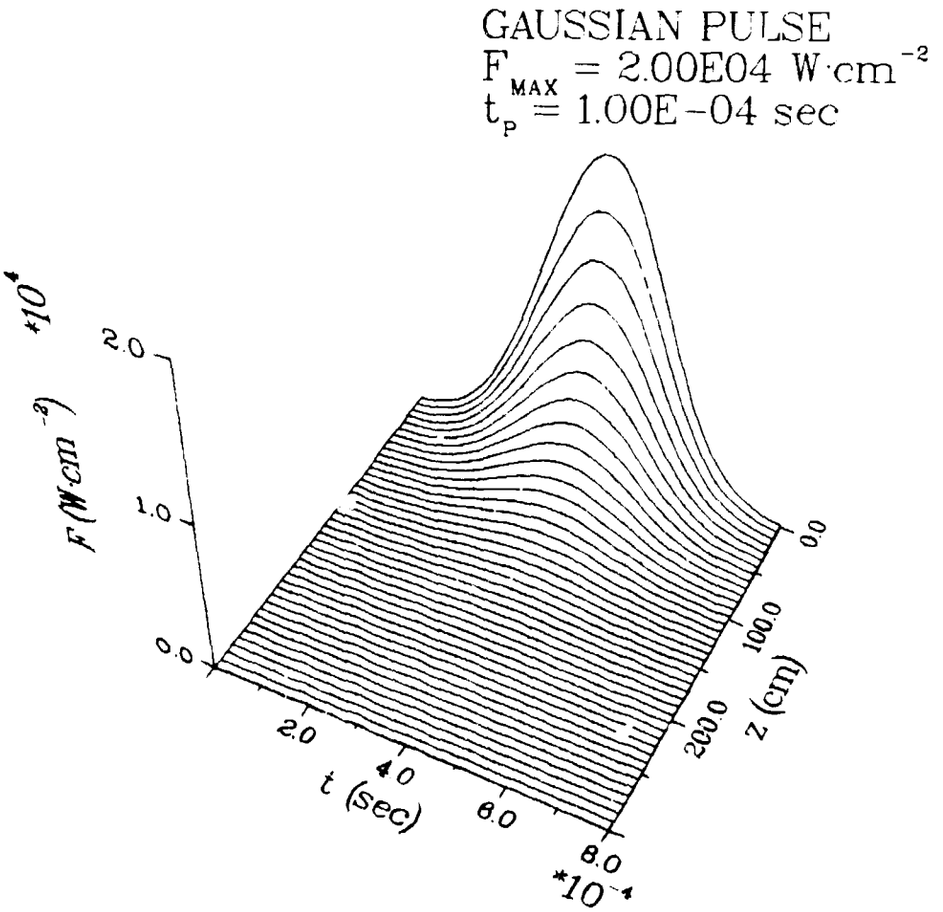

Figure 5. Space-time dependence of beam irradiance on axis for $F_{MAX} = 2\times10^4$ W/cm^2. The propagation is controlled by the Beer-Lambert law and multiple scattering.

as compared to the linear regime; this implies that the filtering effect of the medium tends to be quenched. Because the width of the incident beam decreases as the pulse propagates, the MTF becomes widest for largest path lengths. This type of a paradox does not take place when the propagation is linear.

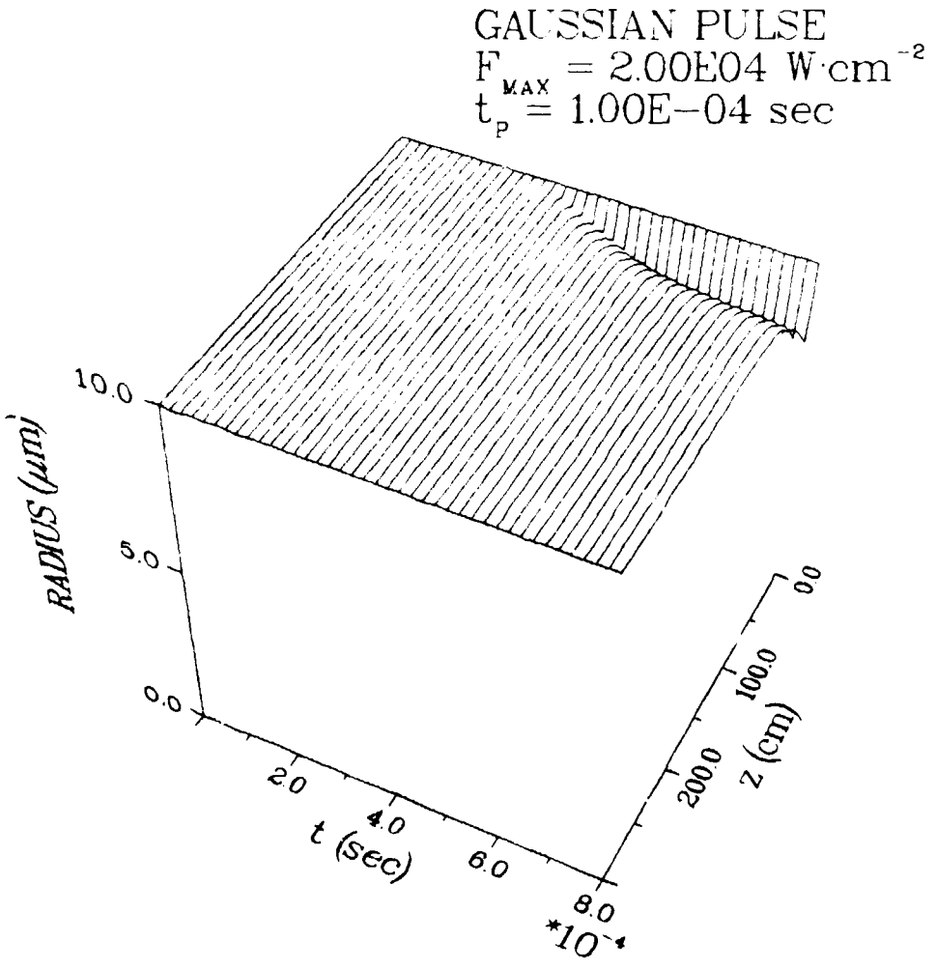

Figure 6. Space-time dependence of the droplet radius on axis for $F_{MAX} = 2\times10^4$ W/cm^2.

6. CONCLUSIONS

We have analyzed the effects of laser beam propagation on imaging in the cases of linear and nonlinear radiative transfer. For low-energy beams, when the propagation is linear and the scattering is forward-peaked, the MTF of the particulate medium has a simple semi-analytic form. As the energy of the beam increases, a host of nonlinear effects can accompany the propagation process; the focus in this paper has been on the effect of vaporization. The nonlinear MTF does not act as a cutoff filter—the width in the spatial frequency domain far exceeds the width of the linear MTF. In addition, by the very nature of nonlinear propagation, the widest MTF corresponds to the largest propagation distance, if the high energy beam is used for imaging. The low-energy probe beam, on the other hand, would propagate through a teneous aerosol cloud, thus experiencing enhanced broadening as the path length increases.

7. REFERENCES

1 A. Ishimaru, "Limitation on image resolution imposed by a random medium," Appl. Opt. 17, 348-352 (1978).

2 Y. Kuga and A. Ishimaru, "Modulation transfer function and image transmission through randomly distributed spherical particles," J. Opt. Soc. Am. A2, 2330-2335 (1985).

3 Y. Kuga and A. Ishimaru, "Modulation transfer function of layered inhomogeneous random media using the small-angle approximation," Appl. Opt. 25, 4382-4385 (1986).

4. A. Zardecki, S. A. W. Gerstl, and R. E. DeKinder, "Two- and three-dimensional radiative transfer in the diffusion approximation," Appl. Opt. 25, 3508–3515 (1986).
5. A. Zardecki, S. A. W. Gerstl, and J. F. Embury, "Multiple scattering effects in spatial frequency filtering," Appl. Opt. 23, 4124–4131 (1984).
6. A. Zardecki, S. A. W. Gerstl, "Significance of multiple scattering in imaging through turbid media," in *Modeling and Simulation of Optoelectronic Systems*, J. Dugan O'Keefe, ed., Proc. SPIE 642, 232–237 (1986).
7. N. S. Kopeika, "Spatial-frequency- and wavelength-dependent effects of aerosols on the atmospheric modulation transfer function," J. Opt. Soc. Am. 72, 1092–1094 (1982).
8. N. S. Kopeika, "Spatial-frequency dependence of scattered light: The atmospheric modulation transfer function resulting from aerosols," J. Opt. Soc. Am. 72, 548–551 (1982).
9. N. S. Kopeika, "Effects of aerosols on imaging through the atmosphere: a review of spatial frequency and wavelength dependent effects," Opt. Eng. 24, 707–712 (1985).
10. A. Zardecki, S. A. W. Gerstl, W. G. Tam, and J. F. Embury, "Image-quality degradation in a turbid medium under partially coherent illumination," J. Opt. Soc. Am. A3, 393–400 (1986).
11. J. Nowakowski, Y. Gorlin, and M. Elbaum, "Effects of target signatures on active tracking," in *Acquisition, Tracking, and Pointing*, R. R. Auelmann and H. L. Richard, eds., Proc SPIE 641, 10–22 (1986).
12. A. Ishimaru, *Wave Propagation and Scattering in Random Media*, pp. 295–325, Academic Press, New York (1978).
13. A. Zardecki and S. A. W. Gerstl, "MultiGaussian phase function model for off-axis laser beam scattering," Appl. Opt. 23, 3000–3004 (1987).
14. R. L. Armstrong, S. A.W. Gerstl, and A. Zardecki, "Nonlinear pulse propagation in the presence of evaporating aerosols," J. Opt. Soc. Am. A2, 1739–1746 (1985).

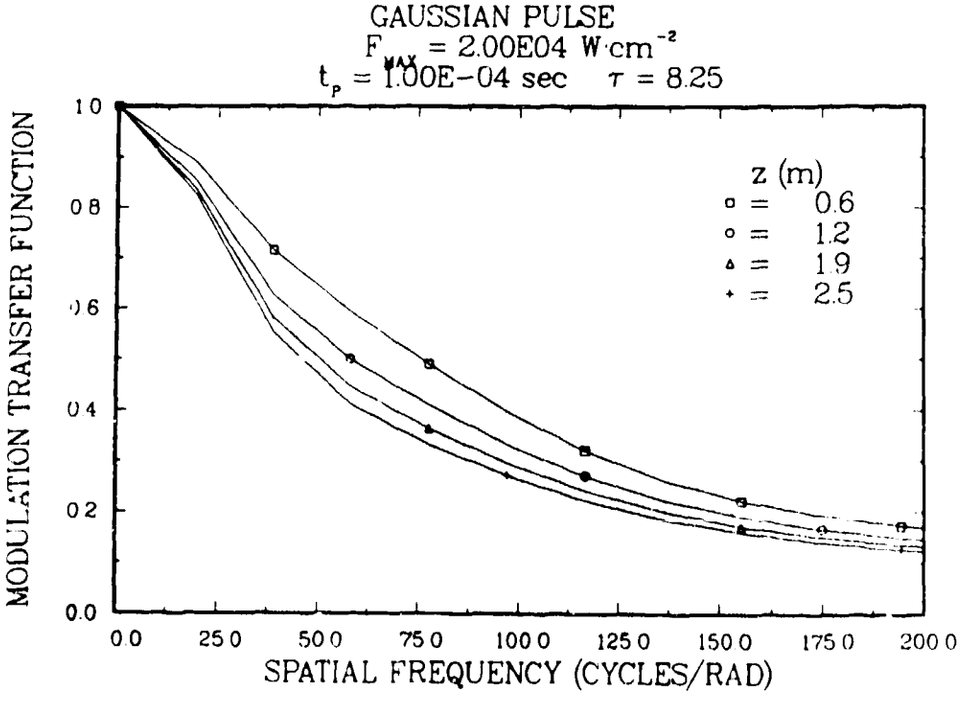

Figure 7. MTF computed from the propagation code for different path lengths; the linear pulse propagation, $F_{MAX} = 2 \times 10^4$ W/cm^2.

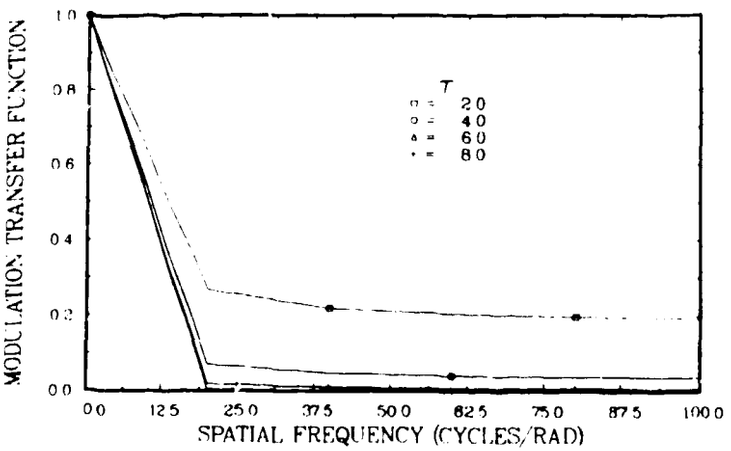

Figure 8. MTF computed from the small-angle approximation formula, Eq. 4. The phase function parameter $\alpha = 16.5\ \text{rad}^{-1}$.

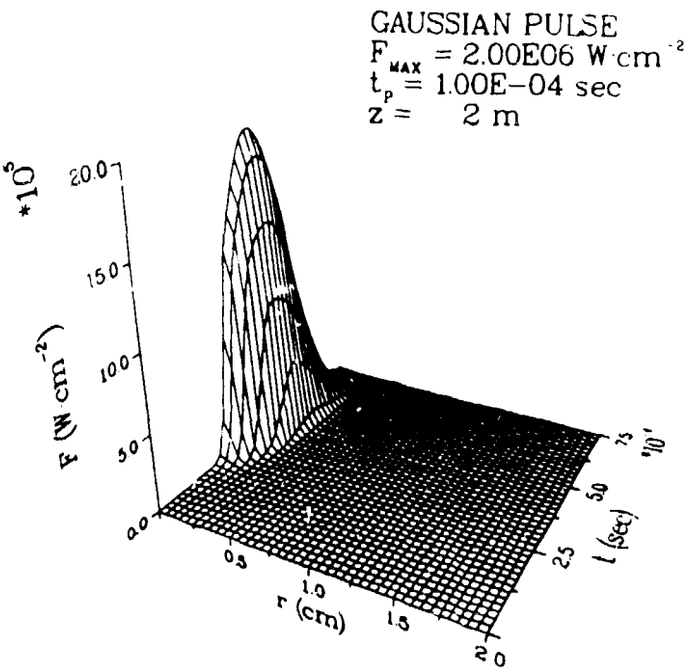

Figure 9. Functional shape at a distance $z = 2$ m. The peak power in the input plane $F_{MAX} = 2 \times 10^6\ \text{W/cm}^2$.

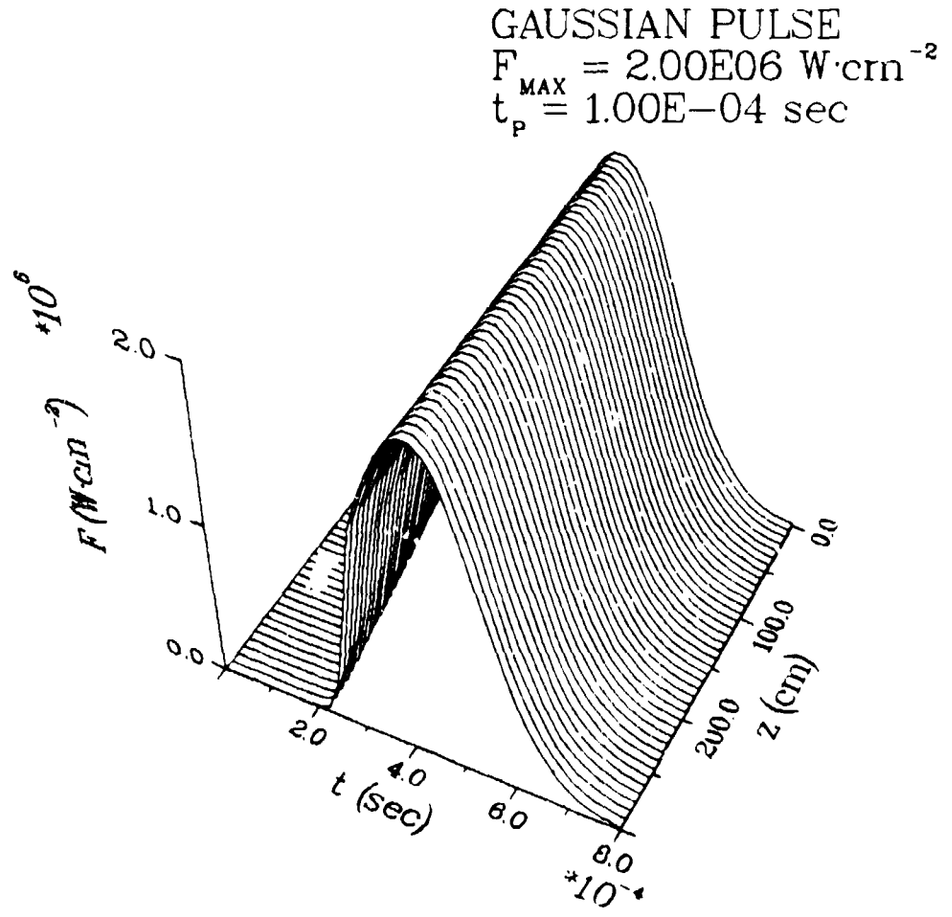

Figure 10. Space-time dependence of beam irradiance on axis for $F_{MAX} = 2 \times 10^6$ W/cm^2. The propagation is controlled by the punch through effect.

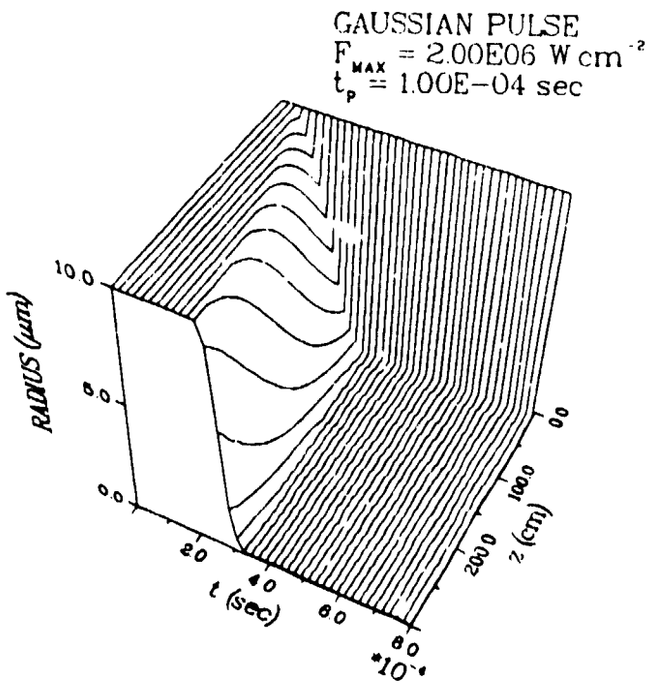

Figure 11. Space-time dependence of the droplet radius on axis for $F_{MAX} = 2\times10^6$ W/cm^2.

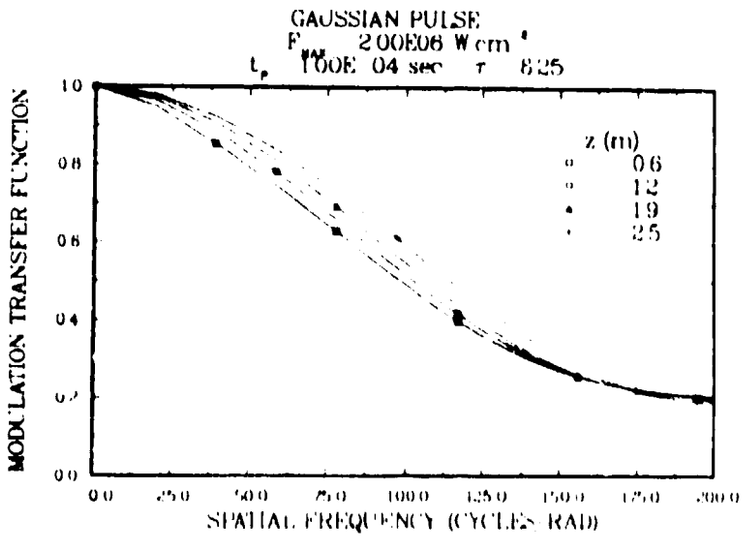

Figure 12. MTF computed from the propagation code for different path lengths; the nonlinear pulse propagation, $F_{MAX} = 2\times10^6$ W/cm^2.